Atmos. Chem. Phys. Discuss., https://doi.org/10.5194/acp-2019-143
Manuscript under review for journal Atmos. Chem. Phys.
Discussion started: 26 April 2019

Atmospheric Chemistry and Physics Discussions

Enrichment of submicron sea salt-containing particles in small cloud droplets based on single particle mass spectrometry

Qinhao Lin[1], Yuxiang Yang[1,2], Yuzhen Fu[1,2], Guohua Zhang[1], Feng Jiang[1,2], Long Peng[1,2], Xiufeng Lian[1,2], Fengxian Liu[1,2,#], Xinhui Bi[1,*], Lei Li[3], Duohong Chen[4], Mei Li[3], Jie Ou[5], Mingjin Tang[1], Xinming Wang[1], Ping'an Peng[1], and Guoying Sheng[1]

[1] State Key Laboratory of Organic Geochemistry and Guangdong Key Laboratory of Environmental Resources Utilization and Protection, Guangzhou Institute of Geochemistry, Chinese Academy of Sciences, Guangzhou 510640, PR China

[2] University of Chinese Academy of Sciences, Beijing 100039, PR China

[3] Institute of Mass Spectrometer and Atmospheric Environment, Jinan University, Guangzhou 510632, PR China

[4] State Environmental Protection Key Laboratory of Regional Air Quality Monitoring, Guangdong Environmental Monitoring Center, Guangzhou 510308, PR China

[5] Shaoguan Environmental Monitoring Center, Shaoguan 512026, PR China

[#] Present at College of Economics and Management, Taiyuan University of Technology, Taiyuan 030024, PR China

*Correspondence to: Xinhui Bi (bixh@gig.ac.cn)

Atmos. Chem. Phys. Discuss., https://doi.org/10.5194/acp-2019-143
Manuscript under review for journal Atmos. Chem. Phys.
Discussion started: 26 April 2019

Atmospheric Chemistry and Physics Discussions

Abstract. The effects of chemical composition and size of sea salt-containing particles on their cloud condensation nuclei (CCN) activity are incompletely understood. We used a ground-based counterflow virtual impactor (GCVI) coupled with a single particle aerosol mass spectrometer (SPAMS) to characterize chemical composition of submicron (dry diameter of 0.2-1.0 μm) and supermicron (dry diameter of 1.0-2.0 μm) sea salt-containing cloud residues (dried cloud droplets) at Mount Nanling, southern China. Seven cut sizes (7.5-14 μm) of cloud droplets were set in the GCVI system. Approximately 20% (by number) of the submicron cloud residues included sea salt-containing particles at the cut size of 7.5 μm, which was significantly higher than the percentages at the cut sizes of 8-14 μm (below 2%). This difference was likely to be involved in the change in the chemical composition. For the cut size of 7.5 μm, nitrate was internally mixed with over 90% of the submicron sea salt-containing cloud residues, which was higher than sulfate (20%), ammonium (below 1%), amines (6%), hydrocarbon organic species (2%), and organic acids (4%). However, nitrate, sulfate, ammonium, amines, hydrocarbon organic species, and organic acids were internally mixed with over 90%, over 80%, 39-84%, 71-86%, 52-90%, and 32-77%, respectively, of the submicron sea salt-containing cloud residues for the cut sizes of 8-14 μm. The proportion of sea salt-containing particles in the supermicron cloud residues generally increased as a function of cut size, and their CCN activity was less influenced by chemical composition. This study highlights the different distribution of the submicron and supermicron sea salt-containing particles in various cloud droplets, which might further influence their atmospheric residence time.

Atmos. Chem. Phys. Discuss., https://doi.org/10.5194/acp-2019-143
Manuscript under review for journal Atmos. Chem. Phys.
Discussion started: 26 April 2019

Atmospheric Chemistry and Physics Discussions

1 Introduction

Atmospheric aerosol particles can directly influence the global radiative forces by scattering and absorbing solar radiation, and can indirectly influence them by serving as cloud condensation nuclei (CCN) (Cochran et al., 2017). The oceans represent one of the largest sources of natural aerosols with an estimated global production rate of 2000-10 000 Tg/yr (Gantt and Meskhidze, 2013). Modeling simulations showed that the indirect radiative forces of sea salt particles were about twice those of the direct forces (Ma et al., 2008). The addition of the sea salt particles over the remote ocean was estimated to enhance its CCN concentration by up to 500% (Pierce and Adams, 2006). The ability of sea salt particles acting as CCN is dependent on their size and chemical composition at a specific supersaturation (Andreae and Rosenfeld, 2008). However, the CCN activity of sea salt particles is still not fully understood due to changes in the chemical composition as a function of the particle size.

Numerous studies have revealed that fresh sea salt particles consist of inorganic salts and biologically produced organic species rather than just sodium chloride (NaCl) (Prather et al., 2013; Quinn et al., 2015; Bertram et al., 2018). The size-resolved chemical composition of fresh sea salt particles is dependent on complex factors including biological sources (e.g., phytoplankton and bacteria), physicochemical (e.g., sea surface active organic species) properties, and wind speeds (Quinn et al., 2015). Previous studies have shown that an increasing fraction of fresh sea salt particles is an internal mixture of inorganic salts (mainly including NaCl) and organic species as a result of the decreasing particle size (Prather et al., 2013; Bertram et al., 2018). However,

this enhancement of organic species in small particles has not always occurred, even in the phytoplankton blooms (Wang et al., 2015). Heterogeneous/multiphase reactions or atmospheric aging processes during transport can further lead to the size-dependent change in the chemical composition of sea salt particles (Dall'Osto et al., 2004; Chi et al., 2015; Bondy et al., 2017). Bondy et al. (2017) found that sulfate was enriched in the submicron sea salt particles while nitrate dominated in the supermicron sea salt particles (Bondy et al., 2017). However, Kirpes et al. (2018) observed that sulfate was also more prevalent than nitrate in supermicron sea salt particles (Kirpes et al., 2018). Additionally, sea salt particles could also react with various organic acids (e.g., oxalate, malonate, and succinate) during transport (Mochida et al., 2003; Laskin et al., 2012). Uncertainty in the formation of secondary species (e.g., sulfate, nitrate, or organic species) would complicate the size-dependent change in the chemical composition of sea salt particles and thus the CCN activity.

Twohy et al. (1989) performed a model to predict size-distribution cloud droplet for submicron ammonium sulfate particles and supermicron sea salt particles, and found that the supermicron sea salt particles enriched in large cloud droplet, and vice versa for the submicron ammonium sulfate particles. The measurement of cloud water observed that secondary species (e.g., sulfate, nitrate, and ammonium) dominated in the 3.5 μm cloud droplets, whereas sodium, calcium, and magnesium dominated in the 16 μm cloud droplets (Monger et al., 1989). Monger et al. (1989) suggested that large cloud droplet mainly consisted of large sea salt or soil dust particles, while small cloud droplets included small secondary species particles. Noone et al. (1988) used a scanning

electron microscope to obtain the morphologies of marine stratus cloud residues (dried cloud droplets) that were collected by a counterflow virtual impactor (CVI) with two cut sizes of 9 and 33 μm (Noone et al., 1988). They speculated that the submicron sulfate-like and supermicron sea salt-like materials dominated in the >9 μm and >33 μm cloud residues, respectively, based on their crystal structures or morphology (Noone et al., 1988). These prior observations showed that the supermicron or giant sea salt-containing particles readily become large cloud droplets, and their CCN behavior was less affected by chemical composition (Andreae and Rosenfeld, 2008; Tao et al., 2012). So far, the study on the submicron sea salt-containing particles in cloud droplet is scarce in the literature. Furthermore, the existence of secondary species (e.g., sulfate, nitrate, or organic species) onto the submicron sea salt-containing particles might significantly impact on cloud drop activation (O'Dowd et al., 1999; Gibson et al., 2006; Nguyen et al., 2017).

In this study, a ground-based CVI (GCVI) combined with an online single particle aerosol mass spectrometer (SPAMS) was used to characterize the chemical composition of sea salt-containing cloud residues at Mount Nanling, southern China. This was performed in the downwind direction from the South China Sea during the study period of May-June, 2017. The main goal of this work was to identify the discrepancies in the chemical compositions of sea salt-containing particles as a function of the cloud droplet cut size (>7.5 μm, >8.0 μm, >8.5 μm, >9.0 μm, >10.0 μm, >11.0 μm, and >14.0 μm were set in the GCVI system). To elucidate the relative contributions of submicron (dry diameter of 0.2-1.0 μm) sea salt-containing particles to size-dependent cloud droplets,

the chemical composition of submicron sea salt-containing particles within various cloud droplet cut sizes was also addressed.

2 Experimental section

2.1 Observation site

The measurements took place from 18 May-11 June, 2017. The time series for the cloud events that are associated with setting the cloud droplet cut sizes is presented in Table S1. The sampling site, which is one National Air Background Monitoring Station, is situated at Mount Nanling, southern China (112°53'56" E, 24°41'56" N at 1,690 m above sea level). The real-time air quality and meteorological parameters are continuously monitored. This station is surrounded by a national park forest (273 km^2), it was minimally affected by local anthropogenic activities. The sampling site is located 50-100 km northeast or north of the Pearl River Delta (PRD) urban agglomeration and 350 km north of the South China Sea (Figure S1). The sampling site is affected by the East Asian summer monsoon system (Ding and Chan, 2005). Generally, air masses would spend some time traveling across the South China Sea and then travel over the PRD region before reaching the sampling site during the summer period. The SO_2, NOx, NH_3, and volatile organic compound emissions in the PRD region are approximately 711, 891, 195, and 1180 kiloton/yr, respectively (Zheng et al., 2009; Zheng et al., 2012). Hence, the sea salt-containing particles that originated from the South China Sea could interact with anthropogenic gaseous pollutants during their movement across the PRD region.

Atmos. Chem. Phys. Discuss., https://doi.org/10.5194/acp-2019-143
Manuscript under review for journal Atmos. Chem. Phys.
Discussion started: 26 April 2019

130

131 **2.2 Instrumentation**

132 A GCVI inlet system (GCVI Model 1205, Brechtel Manufacturing Inc.) was used to
133 sample the cloud droplets with various cut sizes. A lower-limit sampling time of each
134 cut size was 12 hours. The cut size was adjusted by modifying the air velocity in the
135 wind tunnel of the GCVI inlet system (Shingler et al., 2012). It should be noted here
136 that the transmission efficiency increased as the cut size increased (Shingler et al., 2012).
137 The sampled cloud droplets passed through an evaporation chamber to remove the
138 water and the dry residue particles remained. The enrichment factor of the particles that
139 were collected by the GCVI inlet was estimated to range from 6.6 in 7.5 μm to 2.0 in
140 14.0 μm based on theoretical calculations (Shingler et al., 2012). Pekour and Cziczo
141 (2011) observed that the breakthrough of large particles tended to be increase at the
142 lower size cut. In this study, although the number concentration of ambient particles in
143 the GCVI downstream inlet was below 1 cm^3 for different cut sizes during cloud-free
144 events, the large particle breakthrough for the lowest cut size might be overestimation
145 of supermicron cloud residues. In order to reliably identify the presence of clouds, an
146 upper-limit visibility of 3 km and a lower-limit relative humidity (RH) of 95% were set
147 in the GCVI software (Lin et al., 2017). During precipitation periods, the GCVI
148 automatically shut down to protect against interference from raindrops. The cloud
149 residues were subsequently characterized using an online SPAMS (Hexin Analytical
150 Instrument Co., Ltd., Guangzhou, China).

151 The SPAMS conducts the real-time characterization the chemical composition of

aerosol particles using vacuum aerodynamic diameters (d_{va}) between 0.2 and 2.0 μm. The detailed operations of the SPAMS have been described elsewhere (Li et al., 2011). Briefly, aerosol particles are introduced into the SPAMS through a nozzle inlet. The particle velocity is derived from the measurement of two continuous diode Nd:YAG laser beams (532 nm) and is then converted to the particle size (d_{va}). The particles are subsequently desorbed and ionized by a pulsed laser (266 nm). The positive and negative mass spectra that are generated are recorded with the corresponding particle size. The laser pulse energy was regulated at 0.5-0.6 mJ during the whole sampling period. Polystyrene latex spheres (Nanosphere Size Standards, Duke Scientific Corp., Palo Alto) of 0.2-2.0 μm in diameter were used to calibrate the sizes of the detected particles. It should be noted that the particles that were detected by the SPAMS are mostly in the size range of d_{va} 0.2-2.0 μm (Li et al., 2011).

2.3 Screening of sea salt-containing particles

According to prior laboratory and field studies, sea salt-containing particles generally exhibit a set of sodium-related peaks at m/z 23 $[Na]^+$, 46 $[Na_2]^+$, 62 $[Na_2O]^+$, 63 $[Na_2OH]^+$, 81 $[Na_2{}^{35}Cl]^+$, and 83 $[Na_2{}^{37}Cl]^+$ (Dall'Osto et al., 2004; Herich et al., 2009; Prather et al., 2013). Thus, the sea salt-containing particles in this study were identified by the simultaneous existence of peaks at m/z 23, 46, 62, 63, 81, and 83. Because biologically produced organic species (e.g., m/z -26 $[CN]^-$, -42 $[CNO]^-$, or 59 $[NC_3H_9]^+$) were internally mixed with sodium-related peaks (Prather et al., 2013; Sultana et al., 2017), these primary organic species were not intended to define sea salt-containing

particles. Additionally, these organic species might also be produced from secondary aerosol processes (Dall'Osto et al., 2009; Zhang et al., 2012). Therefore, biologically produced organic species that externally mixed with sea salt particles were not considered in the current study. One may expect that chlorine ion peaks at m/z -35 $[^{35}Cl]^-$ or -37 $[^{37}Cl]^-$ in the negative mass spectrum should be considered. Sea salt-containing particles in the atmosphere might not contain chloride due to the complete displacement of chloride by sulfate, nitrate or organic acids during transport (Laskin et al., 2012; Ueda et al., 2014; Arndt et al., 2017). Bondy et al. (2017) also suggested that the identification of sea salt-containing particles without using chloride might give more detailed results the atmospheric aging processes during transport (Bondy et al., 2017). Thus, a total of 30275 sea salt-containing cloud residues including 8317 submicron particles and 21958 supermicron particles were obtained in this study.

3 Results and discussion

3.1 General characteristics

Figure 1 displays the hourly averaged data of the meteorological and air quality parameters during the whole sampling period. The wind direction prevailed southwesterly or southerly during the cloud events and most corresponding air masses originated from the South China Sea (Figure S2), which had abundant moist airflows that were responsible for the formation of the cloud events. The maximum concentrations of $PM_{2.5}$, SO_2, and NO_X were 76 μg/m^3, 2.8 ppb, and 12 ppb, respectively, during the cloud-free periods. When the cloud events occurred, the levels of $PM_{2.5}$, SO_2,

and NO_X clearly decreased, which was indicative of cloud scavenging. The ambient temperature was above 10 ℃ during the whole study period, which allows the formation of liquid cloud droplets.

The average mass spectrum of the sea salt-containing cloud residues during the sampling period is shown in Figure 2. The highest peak at m/z 23 and some small ion peaks at m/z 24 $[Mg]^+$, 39 $[K]^+$, 40 $[Ca]^+$, and 56 $[CaO]^+$ or $[Fe]^+$ were observed in the positive mass spectra. This result was agreement with the previous findings from laboratory and field studies (Guazzotti et al., 2001; Dall'Osto et al., 2004; Gaston et al., 2011; Prather et al., 2013). The significant ion peaks at m/z -46 $[NO_2]^-$ or -62 $[NO_3]^-$ and -97 $[HSO_4]^-$ in the negative mass spectrum represented nitrate and sulfate markers, thus suggesting aged sea salt-containing cloud residues. The presence of organic nitrogen peaks at m/z -26 $[CN]^-$ or -42 $[CNO]^-$ in the negative mass spectrum may be from biologically produced sources or the subsequent accumulation of secondary organic aerosols (Herich et al., 2009; Prather et al., 2013). The small peak areas of other organic species including hydrocarbon organic species (i.e., m/z 15 $[CH_3]^+$, m/z 27 $[C_2H_3]^+$ or m/z 43 $[C_2H_3O]^+$), amines (m/z 59 $[C_3H_9N]^+$ or 86 $[C_5H_{12}N]^+$), or organic acids (m/z -89 oxalate, -103 malonate, or -117 succinate) can also be detected in the sea salt-containing cloud residues (Figure S3).

3.2 Number fraction and chemical composition of sea salt-containing cloud residues

The number fraction (NF) of sea salt-containing particles in the total cloud residues was

dependent on the cut size. The highest NF was observed at the cut size of 7.5 μm (26%, by number), which was followed by 14 μm (17%), and the lowest was for the remaining cut sizes (2-5%) (Figure 3a). These values were almost higher than the NF (2%, by number) of sea salt-containing particles in the total detected particles during cloud-free events. Sea salt-containing particles contributed to approximately 1% (by number) of cloud residues for the cut size of 5.0 μm over Mount Schmücke in central Germany, despite air masses that frequently originated over the Atlantic Ocean (Roth et al., 2016). The proportion reached to 5-10% (by number) for the cut size of 11 μm at the North Slope of Alaska (Zelenyuk et al., 2010). Additionally, the cloud water measurement showed that sea salt-containing particles might accumulate in large cloud droplets (Monger et al., 1989). In contrast to these findings, the number fraction of sea salt-containing cloud residues was not found to increase with increasing in GCVI cut size. Twohy and Anderson (2008) observed an increased NF of sea salt-like cloud residues from coastal areas for the cut size of 20 μm to clean remote oceans for the cut size of 8 μm (Twohy and Anderson, 2008). However, in this study, the enhancement of sea salt-containing cloud residues at the cut size of 7.5 μm unlikely encounters clean condition because of the comparable air quality and meteorological environments for the all cut sizes.

There was a significant difference in the chemical composition of the sea salt-containing cloud residues between the cut size of 7.5 μm and 8-14 μm, as shown in Figure 4. Nitrate was internally mixed with above 90% of the sea salt-containing cloud residues for the all cut sizes. However, notably decreased sulfate (32% versus 87-93%,

by number), ammonium (below 1% versus 21-32%), organic nitrogen (70% versus 87-96%), amines (6% versus 30-64%), hydrocarbon organics (2% versus 22-70%), and organic acids (7% versus 42-76%) internally mixed with the sea salt-containing cloud residues for the cut size of 7.5 μm were compared to 8-14 μm. Roth et al. (2016) found that both sulfate and nitrate were internally mixed with the sea salt-containing cloud residues (Roth et al., 2016). Another study by Zelenyuk et al. (2010) observed that the sea salt-containing cloud residues were composed of four particle types, including fresh NaCl, NaCl internally mixed with nitrate, sulfate and organics (Zelenyuk et al., 2010). In this study, abundant nitrate was found to internally mix with the sea salt-containing cloud residues for the all cut sizes, while sulfate, ammonium, and organic species showed more diversity between the cut sizes of 7.5 μm and 8-14 μm. These differences in the chemical mixtures of sea salt-containing cloud residues dependent on the location suggest that sea salt-containing particles would experience various chemical evolutionary process in the atmosphere and subsequently participate in the formation of cloud droplets. More importantly, together with the enrichment of sea salt-containing cloud residues for the minimum cut size of 7.5 μm that was observed here, this might indicate that the distribution of sea salt-containing cloud residues that were dependent on cloud droplet size is likely influenced by changes in the chemical mixtures of sea salt-containing nuclei. It should be noted here that relative to small cloud droplet, undergoing more time of cloud processing for larger cloud droplet probably increase the in-cloud formation of secondary species, such as sulfate, ammonium or oxalate. The extreme high fraction of nitrate in the sea salt-containing cloud residues for the all cut

sizes was more likely due to the aging processes during atmospheric transport, rather than the in-cloud formation.

It is well-known that the chloride depletion in sea salt-containing particles is mainly due to the formation of secondary species, such as sulfate, nitrate, or organic acids (Laskin et al., 2012; Bondy et al., 2017). The chloride depletion might lower the hygroscopic and CCN properties of sea salt-containing particles (i.e., NaCl) (O'Dowd et al., 1999; Gupta et al., 2015). In this study, chloride was internally mixed with above 80% (by number) of the sea salt-containing cloud residues for the cut sizes of 8-14 μm, which was clearly higher than 51% for the cut size of 7.5 μm. That is, chloride depletion was weakened in the sea salt-containing cloud residues for the cut sizes of 8-14 μm, despite abundant sulfate and organic acids, as was mentioned prior. Based on a laboratory study, Ault et al. (2014) found that organic nitrogen can inhibit the heterogeneous reaction of sea salt-containing particles with HNO_3 (Ault et al., 2014). They used a peak area ratio of chloride to (chloride + nitrate) to estimate the extent of the chloride depletion (Ault et al., 2014). Because the heterogeneous reaction with H_2SO_4, HNO_3, or organic acids and sea salt-containing particles is also present in the atmosphere (Laskin et al., 2012; Chi et al., 2015), a modified peak area ratio (chloride/(chloride + nitrate + sulfate + organic acids)) was applied in the present study. This ratio was found to increase as a function of the increase in the peak area of organic nitrogen, as shown in Figure 5, thereby reflecting the effect of organic nitrogen on the depletion of chloride in sea salt-containing particles in the atmosphere. For the cut sizes of 8-14 μm, abundant organic nitrogen in the sea salt-containing cloud residues likely

lowered the chloride depletion. The ratio was not found to be related with the hydrocarbon organic species. The sensitivity of chloride displacement to the presence of organic species was complex (Ault et al., 2014; Bertram et al., 2018), and further studies must be conducted to identify whether diverse organic species affect the heterogeneous reactivity of individual sea salt-containing particles.

3.3 Submicron sea salt-containing cloud residues

The modeling calculation showed that, compared to supermicron size, submicron sea salt-containing particles may have a dominant contribution to aerosol-cloud interactions when evaluating the indirect impacts of sea salt aerosols, despite the uncertainty in the sizes and concentrations of sea salt aerosols (Gong, 2003). Few field studies focused on the submicron sea salt-containing particles within cloud droplets. In this work, approximately 25% (by number) of the sea salt-containing cloud residues was found to be at the submicron size. It should be noted that the size distribution of the sea salt-containing cloud residues that were detected by the SPAMS cannot represent the real atmosphere because the best detection efficiency of the SPAMS was in the size range of 500-800 nm (Li et al., 2011). The relative contribution of sea salt-containing cloud residues to the cloud residues in the given size range is presented to eliminate the detection efficiency of single particle mass spectrometry (Roth et al., 2016), as shown in Figure 3b. For the cut size of 7.5 μm, 20% (by number) of the submicron cloud residues was found to consist of sea salt-containing particles. This value was prominently higher than that for the cut sizes of 8-14 μm (below 2%, by

306 number). The difference at least reflects that the submicron sea salt-containing particles
307 can increase in the small cloud droplets.

308 The diverse chemical composition of the submicron sea salt-containing cloud
309 residues was found between the cut sizes of 7.5 μm and 8-14 μm. For the cut size of 7.5
310 μm, nitrate was internally mixed with 90% (by number) of the submicron sea salt-
311 containing cloud residues, which was much higher than the fractions of sulfate (20%)
312 and ammonium (below 1%) (Figure 4). It implies that the secondary inorganic species
313 in the submicron sea salt-containing cloud residues for the cut size of 7.5 μm is
314 dominated by nitrate, mostly from the partitioning and heterogeneous/aqueous
315 chemistry of HNO_3 and other precursors (e.g., N_2O_5) in the atmosphere (Chang et al.,
316 2011; Schneider et al., 2017). However, compared to the cut size of 7.5 μm, prominently
317 higher fractions of sulfate (86-94%, by number) and ammonium (38-83%) were found
318 to internally mix with the submicron sea salt-containing cloud residues for the cut sizes
319 of 8-14 μm, thus reflecting more chemically aged processes or more time of cloud
320 processing. This was also supported by the increase in the relative peak areas of these
321 secondary species in the submicron sea salt-containing cloud residues for the cut sizes
322 of 8-14 μm compared to 7.5 μm (Figure S4). The enrichment of sulfate in the submicron
323 sea salt-containing particles has also extensively been reported in the literature
324 (Jourdain et al., 2008; Kelly et al., 2010; Bondy et al., 2017), which is largely a result
325 of the preferential formation of sulfate in submicron particle sizes with great surface
326 area-to-volume ratios (Song and Carmichael, 1999). Initially, fresh sea salt-containing
327 particles generally appear to be alkaline due to carbonate, and they subsequently

328 experience the reactive uptake of SO_2, H_2SO_4, or HNO_3 during transport (Sievering et
329 al., 1999; Alexander et al., 2005). The lack of ammonium suggests that the accumulated
330 secondary acids during transport insufficiently acidize the submicron sea salt-
331 containing cloud residues for the cut size of 7.5 μm, which, in turn, causes the uptake
332 of gaseous NH_3 to fail. In contrast, the accumulated ammonium in the submicron sea
333 salt-containing cloud residues for the cut sizes of 8-14 μm (Figure 4) indicate that the
334 alkaline sea salt-containing cloud residues have been eventually consumed by
335 secondary acids and thus uptake gaseous NH_3 to neutralize these acidic species (Song
336 and Carmichael, 1999). Furthermore, higher number fraction of amines was found to
337 internally mix with the submicron sea salt-containing cloud residues for the cut sizes of
338 8-14 μm compared to 7.5 μm (71-87% versus 6%, by number). Despite the biologically
339 produced amines being internally mixed with fresh sea salt-containing particles
340 (Sultana et al., 2017), a similar feature of ammonium and amines in the submicron sea
341 salt-containing cloud residues that was observed here implies that the presence of
342 amines mainly comes from the partitioning of the gas into the aqueous phase,
343 particularly during cloud processing (Roth et al., 2016; Lin et al., 2017).

344 A laboratory study showed that biologically produced organic nitrogen that internally
345 mixed with freshly sea salt-containing particles was found to increase in the submicron
346 size range (Prather et al., 2013). This likely led to the enrichment of organic nitrogen
347 (58%, by number) relative to hydrocarbon organic species (2%) or organic acids (4%)
348 in the submicron sea salt-containing cloud residues for the cut size of 7.5 μm (Figure
349 4). Meanwhile, for the cut sizes of 8-14 μm, higher fractions of organic nitrogen (80-

94%, by number), hydrocarbon organic species (52-90%), and organic acids (32-77%) were observed (Figure 4), indicative of the more chemically aged processes, as mentioned above. Note that magnesium and calcium internally mixed with above 85% (by number) and above 88%, respectively, of the submicron sea salt-containing cloud residues for the cut sizes of 8-14 μm might increase the presence of organic nitrogen due to the probable complexation with organic species and these cations (Bertram et al., 2018). Hydrocarbon organic particle types coupled with the peak area Mg >> Na can be produced from biological sources in seawater, but they were externally mixed with fresh submicron sea salt-containing particles (Sultana et al., 2017). Thus, the abundant hydrocarbon organics that were observed here mostly originated from accumulation during transport. The uptake of gaseous organic acids or the organic acids that formed through heterogeneous reactions were responsible for the increased organic acids that are presented herein (Mochida et al., 2003; Sullivan and Prather, 2007). Petters and Kreidenweis (2007) described the CCN activity of multicomponent aerosol particles using a single parameter (κ) as follows (Petters and Kreidenweis, 2007):

$$\kappa = \varepsilon_{org} * \kappa_{org} + \varepsilon_{inorg} * \kappa_{inorg}$$

where ε_{org} and ε_{inorg} represent the bulk volume fractions of organic and inorganic species, respectively, and κ_{org} (generally below 0.5 for organic species) and κ_{inorg} (1.28 for NaCl, 0.88 for $NaNO_3$, 0.80 for Na_2SO_4, 0.67 for NH_4NO_3, and 0.61 for $(NH_4)_2SO_4$) refer to the CCN-derived hygroscopicity parameters of the organic and inorganic species, respectively (Petters and Kreidenweis, 2007). Relative to the cut sizes of 8-14 μm, the reduction of organic species in the submicron sea salt-containing cloud residues for the

cut size of 7.5 μm is likely to increase κ and hence CCN property. This might lead to the enrichment of submicron sea salt-containing particles in small cloud droplets. We cannot preclude that the decreased organic species of the submicron sea salt-containing particles for the cut size of 7.5 μm might be also due to the undergoing less time of cloud processing relative to other cut sizes. Further study need to compare the contribution of aging degree during transport and duration time of cloud process to the content of secondary species.

3.4 Supermicron sea salt-containing cloud residues

With the increasing cut size, the supermicron (dry diameter of 1.0-2.0 μm) cloud residues were observed to include of more sea salt-containing particles (Figure 3b). For instance, up to 70% of the supermicron cloud residues were found to consist of sea salt-containing particles at the maximum cut size of 14 μm. The enrichment of the large supermicron or giant sea salt-containing particles in large cloud droplets has also been reported in previous studies (Noone et al., 1988; Twohy et al., 1989; Tao et al., 2012). Nitrate was internally mixed with above 90% (by number) of the supermicron sea salt-containing cloud residues for the all the cut sizes (Figure 4). Similar to the submicron particle size, the proportions of sulfate, ammonium, and organic species in supermicron sea salt-containing cloud residues for the cut size of 7.5 μm were lower than those for the cut sizes of 8-14 μm (Figure 4). It was likely that the enrichment of the supermicron sea salt-containing cloud residues in the large cloud droplet, and their CCN activity was less affected by the change in the chemical composition. For coarse or giant nuclei (dry

particle size > 1 μm), their CCN abilities were dependent on their size rather than their chemical composition (Andreae and Rosenfeld, 2008; Tao et al., 2012). Hudson and Rogers (1986) also found that large nuclei increased in large cloud droplets due to lower critical supersaturation of larger nuclei compared to smaller nuclei (Hudson and Rogers, 1986).

4 Atmospheric implications and conclusion

This work focused on the size-resolved chemical composition of sea salt-containing cloud residues as a function of the cloud droplet cut size. Nitrate internally mixed with above 95% (by number) of the sea salt-containing cloud residues for all cut sizes emphasized that the sea salt-containing nuclei had undergone chemical evolution during transport. For simplicity, modeling simulations assumed that the externally mixed NaCl and secondary species (e.g., sulfate) mode or pure NaCl instead of sea salt aerosols was used to predict the size-dependent cloud droplet chemistry or the residence time of sea salt aerosols in the atmosphere (Twohy et al., 1989; Gong et al., 2002; Ma et al., 2008). The change in chemical composition of the submicron sea salt-containing particles might have an impact on their CCN activity. Our result showed that the reduction of organic species in the submicron sea salt-containing cloud residues for the cut size of 7.5 μm is likely to increase CCN activity, leading to the enrichment of the submicron sea salt-containing particles. The resulting effect might prolong the residence time of submicron sea salt-containing aerosols in the atmosphere. This differed from the supermicron sea salt-containing particles, which readily become large

cloud droplet, consistent with the previous measurements (Noone et al., 1988; Yuan et al., 2008). More work is needed to evaluate the contribution of atmospheric aged processes to the change in the chemical composition that is associated with the CCN activity of sea salt-containing particles, particularly in the submicron size range.

Author contribution

XHB, GHZ, and QHL planned and designed the experimental setup. YXY, YZF, LP, FJ, XFL, FXL, and JO performed the atmospheric measurement and collected the data. QHL and XHB analyzed the data and wrote the manuscript. LL, DHC, ML, MJT, XMW, PAP, and GYS contributed comments.

Acknowledgements

This work was supported by the National Key Research and Development Program of China (2017YFC0210104), the National Nature Science Foundation of China (No. 41877307, 41775124 and 41805103), the Foundation for Leading Talents of the Guangdong Province Government, and the State Key Laboratory of Organic Geochemistry (SKLOG2016-A05). The authors also acknowledge the NOAA Air Resources Laboratory for the provision of the HYSPLIT transport and dispersion model and READY website (http://ready.arl.noaa.gov) used in this publication.

References

Alexander, B., Park, R. J., Jacob, D. J., Li, Q. B., Yantosca, R. M., Savarino, J., Lee, C.

C. W., and Thiemens, M. H.: Sulfate formation in sea-salt aerosols: Constraints from oxygen isotopes, J. Geophys. Res.-Atmos., 110, D10307, https://doi.org/10.1029/2004jd005659, 2005.

Andreae, M. O., and Rosenfeld, D.: Aerosol-cloud-precipitation interactions. Part 1. The nature and sources of cloud-active aerosols, Earth-Sci. Rev., 89, 13-41, https://doi.org/10.1016/j.earscirev.2008.03.001, 2008.

Arndt, J., Sciare, J., Mallet, M., Roberts, G. C., Marchand, N., Sartelet, K., Sellegri, K., Dulac, F., Healy, R. M., and Wenger, J. C.: Sources and mixing state of summertime background aerosol in the north-western Mediterranean basin, Atmos. Chem. Phys., 17, 6975-7001, https://doi.org/10.5194/acp-17-6975-2017, 2017.

Ault, A. P., Guasco, T. L., Baltrusaitis, J., Ryder, O. S., Trueblood, J. V., Collins, D. B., Ruppel, M. J., Cuadra-Rodriguez, L. A., Prather, K. A., and Grassian, V. H.: Heterogeneous reactivity of nitric acid with nascent sea spray aerosol: Large differences observed between and within individual particles, J. Phys. Chem. Lett., 5, 2493-2500, https://doi.org/10.1021/jz5008802, 2014.

Bertram, T. H., Cochran, R. E., Grassian, V. H., and Stone, E. A.: Sea spray aerosol chemical composition: Elemental and molecular mimics for laboratory studies of heterogeneous and multiphase reactions, Chem. Soc. Rev., 47, 2374-2400, https://doi.org/10.1039/C7CS00008A, 2018.

Bondy, A. L., Wang, B., Laskin, A., Craig, R. L., Nhliziyo, M. V., Bertman, S. B., Pratt, K. A., Shepson, P. B., and Ault, A. P.: Inland sea spray aerosol transport and incomplete chloride depletion: Varying degrees of reactive processing observed

during SOAS, Environ. Sci. Technol., 51, 9533-9542, https://doi.org/10.1021/acs.est.7b02085, 2017.

Chang, W. L., Bhave, P. V., Brown, S. S., Riemer, N., Stutz, J., and Dabdub, D.: Heterogeneous atmospheric chemistry, ambient measurements, and model calculations of N_2O_5: A review, Aerosol Sci. Tech., 45, 665-695, https://doi.org/10.1080/02786826.2010.551672, 2011.

Chi, J. W., Li, W. J., Zhang, D. Z., Zhang, J. C., Lin, Y. T., Shen, X. J., Sun, J. Y., Chen, J. M., Zhang, X. Y., Zhang, Y. M., and Wang, W. X.: Sea salt aerosols as a reactive surface for inorganic and organic acidic gases in the Arctic troposphere, Atmos. Chem. Phys., 15, 11341-11353, https://doi.org/10.5194/acp-15-11341-2015, 2015.

Cochran, R. E., Ryder, O. S., Grassian, V. H., and Prather, K. A.: Sea spray aerosol: The chemical link between the oceans, atmosphere, and climate, Accounts Chem. Res., 50, 599-604, https://doi.org/10.1021/acs.accounts.6b00603, 2017.

Dadashazar, H., Wang, Z., Crosbie, E., Brunke, M., Zeng, X. B., Jonsson, H., Woods, R. K., Flagan, R. C., Seinfeld, J. H., and Sorooshian, A.: Relationships between giant sea salt particles and clouds inferred from aircraft physicochemical data, J. Geophys. Res.-Atmos., 122, 3421-3434, https://doi.org/10.1002/2016JD026019, 2017.

Dall'Osto, M., Beddows, D. C. S., Kinnersley, R. P., Harrison, R. M., Donovan, R. J., and Heal, M. R.: Characterization of individual airborne particles by using aerosol time-of-flight mass spectrometry at Mace Head, Ireland, J. Geophys. Res.-Atmos., 109, D21302, https://doi.org/10.1029/2004jd004747, 2004.

482 Dall'Osto, M., Harrison, R., Coe, H., and Williams, P.: Real-time secondary aerosol
483 formation during a fog event in London, Atmos. Chem. Phys., 9, 2459-2469,
484 https://doi.org/10.5194/acp-9-2459-2009, 2009.
485 Ding, Y., and Chan, J. C. L.: The East Asian summer monsoon: An overview, Meteorol.
486 Atmos. Phys., 89, 117-142, https://doi.org/10.1007/s00703-005-0125-z, 2005.
487 Gantt, B., and Meskhidze, N.: The physical and chemical characteristics of marine
488 primary organic aerosol: A review, Atmos. Chem. Phys., 13, 3979-3996,
489 https://doi.org/10.5194/acp-13-3979-2013, 2013.
490 Gaston, C. J., Furutani, H., Guazzotti, S. A., Coffee, K. R., Bates, T. S., Quinn, P. K.,
491 Aluwihare, L. I., Mitchell, B. G., and Prather, K. A.: Unique ocean-derived
492 particles serve as a proxy for changes in ocean chemistry, J. Geophys. Res.-Atmos.,
493 116, D18310, https://doi.org/10.1029/2010JD015289, 2011.
494 Gibson, E. R., Hudson, P. K., and Grassian, V. H.: Physicochemical properties of nitrate
495 aerosols: Implications for the atmosphere, J. Phys. Chem. A, 110, 11785-11799,
496 https://doi.org/10.1021/jp063821k, 2006.
497 Gong, S. L., Barrie, L. A., and Lazare, M.: Canadian Aerosol Module (CAM): A size-
498 segregated simulation of atmospheric aerosol processes for climate and air quality
499 models 2. Global sea-salt aerosol and its budgets, J. Geophys. Res.-Atmos., 107,
500 D24, 4779, https://doi.org/10.1029/2001jd002004, 2002.
501 Gong, S. L.: A parameterization of sea-salt aerosol source function for sub- and super-
502 micron particles, Global Biogeochem. Cycles, 17, 1097,
503 https://doi.org/10.1029/2003gb002079, 2003.

504 Guazzotti, S. A., Coffee, K. R., and Prather, K. A.: Continuous measurements of size-
505 resolved particle chemistry during INDOEX-intensive field phase 99, J. Geophys.
506 Res.-Atmos., 106, 28607-28627, https://doi.org/10.1029/2001jd900099, 2001.
507 Gupta, D., Kim, H., Park, G., Li, X., Eom, H. J., and Ro, C. U.: Hygroscopic properties
508 of NaCl and $NaNO_3$ mixture particles as reacted inorganic sea-salt aerosol
509 surrogates, Atmos. Chem. Phys., 15, 3379-3393, https://doi.org/10.5194/acp-15-
510 3379-2015, 2015.
511 Herich, H., Kammermann, L., Friedman, B., Gross, D. S., Weingartner, E., Lohmann,
512 U., Spichtinger, P., Gysel, M., Baltensperger, U., and Cziczo, D. J.: Subarctic
513 atmospheric aerosol composition: 2. Hygroscopic growth properties, J. Geophys.
514 Res.-Atmos., 114, D13204, https://doi.org/10.1029/2008jd011574, 2009.
515 Hudson, J. G., and Rogers, C. F.: Relationship between critical supersaturation and
516 cloud droplet size-implications for cloud mixing processes, J. Atmos. Sci., 43,
517 2341-2359, https://doi.org/10.1175/1520-0469(1986)043<2341:Rbcsac>2.0.Co;2,
518 1986.
519 Jourdain, B., Preunkert, S., Cerri, O., Castebrunet, H., Udisti, R., and Legrand, M.:
520 Year-round record of size-segregated aerosol composition in central Antarctica
521 (Concordia station): Implications for the degree of fractionation of sea-salt
522 particles, J. Geophys. Res.-Atmos., 113, D14308,
523 https://doi.org/10.1029/2007jd009584, 2008.
524 Kelly, J., Bhave, P., Nolte, C., Shankar, U., and Foley, K.: Simulating emission and
525 chemical evolution of coarse sea-salt particles in the Community Multiscale Air

Quality (CMAQ) model, Geosci. Model Dev., 3, 257-273, https://doi.org/10.5194/gmd-3-257-2010, 2010.

Kirpes, R. M., Bondy, A. L., Bonanno, D., Moffet, R. C., Wang, B., Laskin, A., Ault, A. P., and Pratt, K. A.: Secondary sulfate is internally mixed with sea spray aerosol and organic aerosol in the winter Arctic, Atmos. Chem. Phys., 18, 3937-3949, https://doi.org/10.5194/acp-18-3937-2018, 2018.

Laskin, A., Moffet, R. C., Gilles, M. K., Fast, J. D., Zaveri, R. A., Wang, B., Nigge, P., and Shutthanandan, J.: Tropospheric chemistry of internally mixed sea salt and organic particles: Surprising reactivity of NaCl with weak organic acids, J. Geophys. Res.-Atmos., 117, D15302, https://doi.org/10.1029/2012jd017743, 2012.

Li, L., Huang, Z., Dong, J., Li, M., Gao, W., Nian, H., Fu, Z., Zhang, G., Bi, X., Cheng, P., and Zhou, Z.: Real time bipolar time-of-flight mass spectrometer for analyzing single aerosol particles, Int. J. Mass Spectrom., 303, 118-124, https://doi.org/10.1016/j.ijms.2011.01.017, 2011.

Lin, Q., Zhang, G., Peng, L., Bi, X., Wang, X., Brechtel, F. J., Li, M., Chen, D., Peng, P., amp, apos, an, Sheng, G., and Zhou, Z.: In situ chemical composition measurement of individual cloud residue particles at a mountain site, southern China, Atmos. Chem. Phys., 17, 8473-8488, https://doi.org/10.5194/acp-17-8473-2017, 2017.

Ma, X., Von Salzen, K., and Li, J.: Modelling sea salt aerosol and its direct and indirect effects on climate, Atmos. Chem. Phys., 8, 1311-1327,

https://doi.org/10.5194/acp-8-1311-2008, 2008.

Mochida, M., Umemoto, N., Kawamura, K., and Uematsu, M.: Bimodal size distribution of C_2–C_4 dicarboxylic acids in the marine aerosols, Geophys. Res. Lett., 30, 1672, https://doi.org/10.1029/2003GL017451, 2003.

Monger, J. W., Jr, J. C., Jr, B. D., and Hoffmann, M. R.: Chemical composition of coastal stratus clouds: Dependence on droplet size and distance from the coast, Atmos. Environ., 23, 2305-2320, https://doi.org/10.1016/0004-6981(89)90192-3, 1989.

Nguyen, Q.T., Kjaer, K.H., Kling, K.I., Boesen, T., and Bilde, M.: Impact of fatty acid coating on the CCN activity of sea salt particles, Tellus B, 69, 1304064, https://doi.org/10.1080/16000889.2017.1304064, 2017.

Noone, K. J., Charlson, R. J., Covert, D. S., Ogren, J. A., and Heintzenberg, J.: Cloud droplets: Solute concentration is size dependent, J. Geophys. Res.-Atmos., 93, 9477-9482, https://doi.org/10.1029/JD093iD08p09477, 1988.

O'Dowd, C. D., Lowe, J. A., and Smith, M. H.: Coupling sea-salt and sulphate interactions and its impact on cloud droplet concentration predictions, Geophys. Res. Lett., 26, 1311-1314, https://doi.org/10.1029/1999gl900231, 1999.

Petters, M. D., and Kreidenweis, S. M.: A single parameter representation of hygroscopic growth and cloud condensation nucleus activity, Atmos. Chem. Phys., 7, 1961-1971, https://doi.org/10.5194/acp-7-1961-2007, 2007.

Pierce, J. R., and Adams, P. J.: Global evaluation of CCN formation by direct emission of sea salt and growth of ultrafine sea salt, J. Geophys. Res.-Atmos., 111, D06203,

570 https://doi.org/10.1029/2005jd006186, 2006.

571 Prather, K. A., Bertram, T. H., Grassian, V. H., Deane, G. B., Stokes, M. D., Demott, P.
572 J., Aluwihare, L. I., Palenik, B. P., Azam, F., and Seinfeld, J. H.: Bringing the
573 ocean into the laboratory to probe the chemical complexity of sea spray aerosol, P.
574 Natl. Acad. Sci. USA, 110, 7550-7555, https://doi.org/10.1073/pnas.1300262110,
575 2013.

576 Quinn, P. K., Collins, D. B., Grassian, V. H., Prather, K. A., and Bates, T. S.: Chemistry
577 and related properties of freshly emitted sea spray aerosol, Chem. Rev., 115, 4383-
578 4399, https://doi.org/10.1021/cr500713g, 2015.

579 Roth, A., Schneider, J., Klimach, T., Mertes, S., van Pinxteren, D., Herrmann, H., and
580 Borrmann, S.: Aerosol properties, source identification, and cloud processing in
581 orographic clouds measured by single particle mass spectrometry on a central
582 European mountain site during HCCT-2010, Atmos. Chem. Phys., 16, 505-524,
583 https://doi.org/10.5194/acp-16-505-2016, 2016.

584 Schneider, J., Mertes, S., van Pinxteren, D., Herrmann, H., and Borrmann, S.: Uptake
585 of nitric acid, ammonia, and organics in orographic clouds: mass spectrometric
586 analyses of droplet residual and interstitial aerosol particles, Atmos. Chem. Phys.,
587 17, 1571-1593, https://doi.org/10.5194/acp-17-1571-2017, 2017.

588 Shingler, T., Dey, S., Sorooshian, A., Brechtel, F. J., Wang, Z., Metcalf, A., Coggon, M.,
589 Mülmenstädt, J., Russell, L. M., Jonsson, H. H., and Seinfeld, J. H.:
590 Characterisation and airborne deployment of a new counterflow virtual impactor
591 inlet, Atmos. Meas. Tech., 5, 1259-1269, https://doi.org/10.5194/amt-5-1259-

592 2012, 2012.

593 Sievering, H., Lerner, B., Slavich, J., Anderson, J., Pósfai, M., and Cainey, J.: O_3
594 oxidation of SO_2 in sea-salt aerosol water: Size distribution of non-sea-salt sulfate
595 during the First Aerosol Characterization Experiment (ACE 1), J. Geophys. Res.-
596 Atmos., 104, 21707-21717, https://doi.org/10.1029/1998jd100086, 1999.

597 Song, C. H., and Carmichael, G. R.: The aging process of naturally emitted aerosol
598 (sea-salt and mineral aerosol) during long range transport, Atmos. Environ., 33,
599 2203-2218, https://doi.org/10.1016/S1352-2310(98)00301-X, 1999.

600 Sullivan, R. C., and Prather, K. A.: Investigations of the diurnal cycle and mixing state
601 of oxalic acid in individual particles in Asian aerosol outflow, Environ. Sci.
602 Technol., 41, 8062-8069, https://doi.org/10.1021/es071134g. 2007.

603 Sultana, C. M., Collins, D. B., and Prather, K. A.: Effect of structural heterogeneity in
604 chemical composition on online single-particle mass spectrometry analysis of sea
605 spray aerosol particles, Environ. Sci. Technol., 51, 3660-3668,
606 https://doi.org/10.1021/acs.est.6b06399, 2017.

607 Tao, W. K., Chen, J. P., Li, Z. Q., Wang, C., and Zhang, C. D.: Impact of aerosols on
608 convective clouds and precipitation, Rev. Geophys., 50, RG2001,
609 https://doi.org/10.1029/2011rg000369, 2012.

610 Twohy, C. H., Austin, P. H., and Charlson, R. J.: Chemical consequences of the initial
611 diffusional growth of cloud droplets: A clean marine case, Tellus B, 41, 51-60,
612 https://doi.org/10.1111/j.1600-0889.1989.tb00124.x, 1989.

613 Twohy, C. H., and Anderson, J. R.: Droplet nuclei in non-precipitating clouds:

614 Composition and size matter, Environ. Res. Lett., 3, 045002,
615 https://doi.org/10.1088/1748-9326/3/4/045002, 2008.
616 Ueda, S., Hirose, Y., Miura, K., and Okochi, H.: Individual aerosol particles in and
617 below clouds along a Mt. Fuji slope: Modification of sea-salt-containing particles
618 by in-cloud processing, Atmos. Res., 137, 216-227,
619 https://doi.org/10.1016/j.atmosres.2013.10.011, 2014.
620 Wang, X., Sultana, C. M., Trueblood, J., Hill, T. C., Malfatti, F., Lee, C., Laskina, O.,
621 Moore, K. A., Beall, C. M., McCluskey, C. S., Cornwell, G. C., Zhou, Y., Cox, J.
622 L., Pendergraft, M. A., Santander, M. V., Bertram, T. H., Cappa, C. D., Azam, F.,
623 DeMott, P. J., Grassian, V. H., and Prather, K. A.: Microbial control of sea spray
624 aerosol composition: A tale of two blooms, ACS Central Sci., 1, 124-131,
625 https://doi.org/10.1021/acscentsci.5b00148, 2015.
626 Yuan, T., Li, Z., Zhang, R., and Fan, J.: Increase of cloud droplet size with aerosol
627 optical depth: An observation and modeling study, J. Geophys. Res.-Atmos., 113,
628 D04201, https://doi.org/10.1029/2007jd008632, 2008.
629 Zelenyuk, A., Imre, D., Earle, M., Easter, R., Korolev, A., Leaitch, R., Liu, P.,
630 Macdonald, A. M., Ovchinnikov, M., and Strapp, W.: In situ characterization of
631 cloud condensation nuclei, interstitial, and background particles using the single
632 particle mass spectrometer, SPLAT II†, Anal. Chem., 82, 7943-7951,
633 https://doi.org/10.1021/ac1013892, 2010.
634 Zhang, G., Bi, X., Chan, L. Y., Li, L., Wang, X., Feng, J., Sheng, G., Fu, J., Li, M., and
635 Zhou, Z.: Enhanced trimethylamine-containing particles during fog events

detected by single particle aerosol mass spectrometry in urban Guangzhou, China, Atmos. Environ., 55, 121-126, https://doi.org/10.1016/j.atmosenv.2012.03.038, 2012.

Zheng, J., Zhang, L., Che, W., Zheng, Z., and Yin, S.: A highly resolved temporal and spatial air pollutant emission inventory for the Pearl River Delta region, China and its uncertainty assessment, Atmos. Environ., 43, 5112-5122, https://doi.org/10.1016/j.atmosenv.2009.04.060, 2009.

Zheng, J., Yin, S. S., Kang, D. W., Che, W. W., and Zhong, L. J.: Development and uncertainty analysis of a high-resolution NH_3 emissions inventory and its implications with precipitation over the Pearl River Delta region, China, Atmos. Chem. Phys., 12, 7041-7058, https://doi.org/10.5194/acp-12-7041-2012, 2012.

Figure captions:

Figure 1. The hourly averaged data of meteorological and air quality parameters.

Figure 2. The averaged mass spectrum of the sea salt-containing cloud residues.

Figure 3. Number fraction or counts of sea salt-containing cloud residues as a function of the cut size (a) and the relative contribution of sea salt-containing cloud residues to the total cloud residues in the given size range (b).

Figure 4. Mixed fractions of inorganic and organic species in the sea salt-containing cloud residues. The inorganic species include sulfate (m/z -97), nitrate (m/z -46 or -62), chloride (m/z -35 or -37), ammonium (m/z 18), magnesium (m/z 24), and calcium (m/z 40). The organic species include organic nitrogen (m/z -26 or -42), amines (m/z 59 or 86), CH_3 (m/z 15), C_2H_3 (m/z 27), C_2H_3O (m/z 43), oxalate (m/z -89), malonate (m/z -103), and succinate (m/z -117).

Figure 5. Ratios as a function of the organic nitrogen (m/z -26 or -42) peak area. The ratios refer to the chloride (m/z -35 or -37) peak area divided by the sum of the sulfate (m/z -97), nitrate (m/z -46 or -62), organic acids (m/z -89, -103, or -117), and chloride peak areas, as explained in the text.

Atmos. Chem. Phys. Discuss., https://doi.org/10.5194/acp-2019-143
Manuscript under review for journal Atmos. Chem. Phys.
Discussion started: 26 April 2019

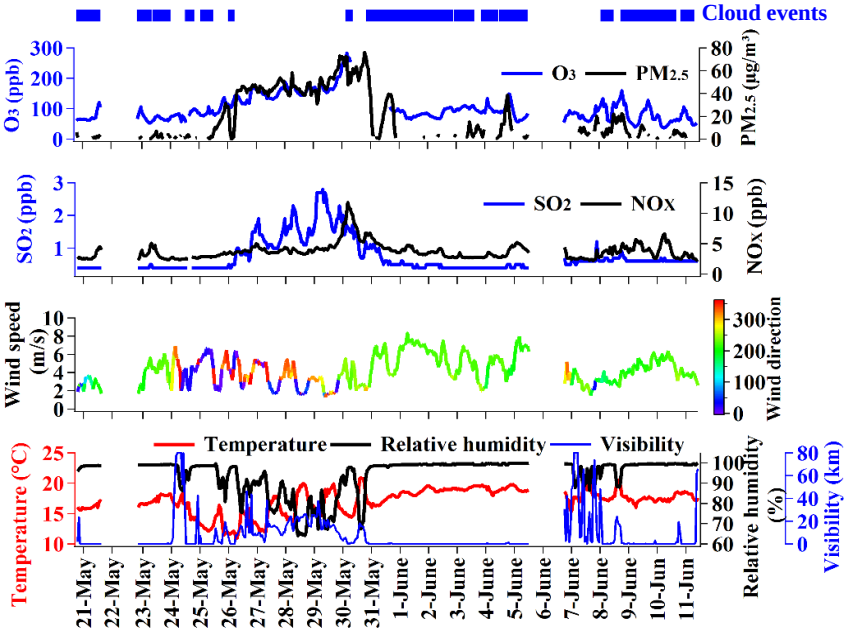

664 Figure 1

Atmos. Chem. Phys. Discuss., https://doi.org/10.5194/acp-2019-143
Manuscript under review for journal Atmos. Chem. Phys.
Discussion started: 26 April 2019

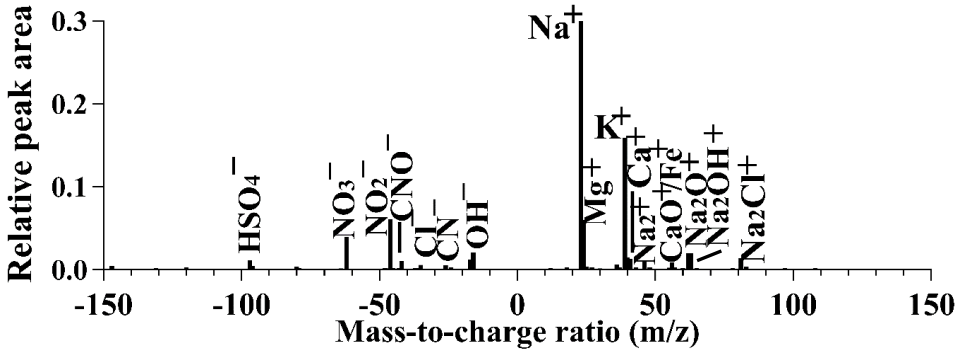

665

666 Figure 2

Atmos. Chem. Phys. Discuss., https://doi.org/10.5194/acp-2019-143
Manuscript under review for journal Atmos. Chem. Phys.
Discussion started: 26 April 2019

Atmospheric Chemistry and Physics Discussions

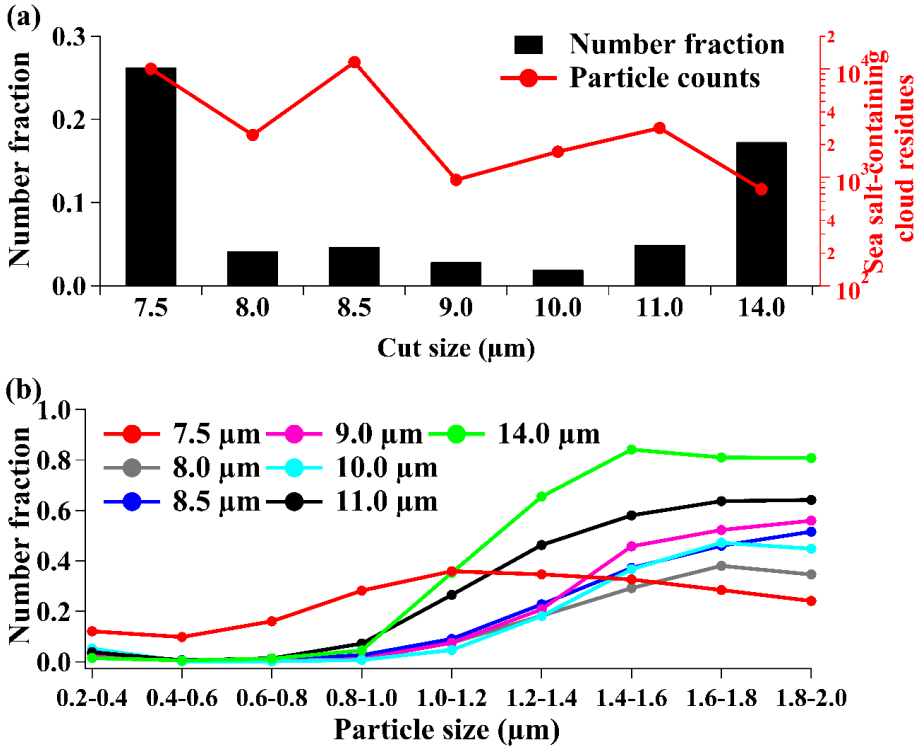

667

668 Figure 3

Atmos. Chem. Phys. Discuss., https://doi.org/10.5194/acp-2019-143
Manuscript under review for journal Atmos. Chem. Phys.
Discussion started: 26 April 2019

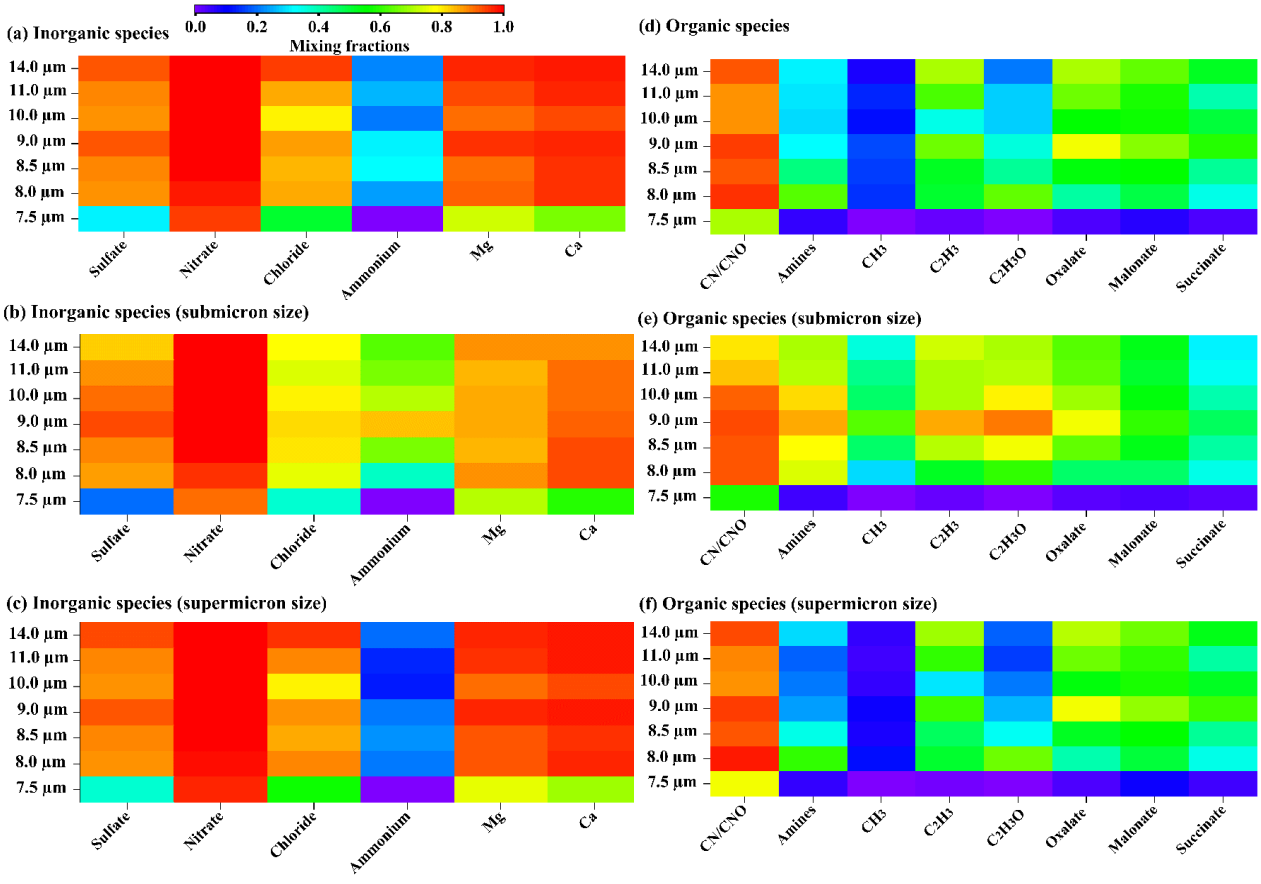

669

670 Figure 4

Atmos. Chem. Phys. Discuss., https://doi.org/10.5194/acp-2019-143
Manuscript under review for journal Atmos. Chem. Phys.
Discussion started: 26 April 2019

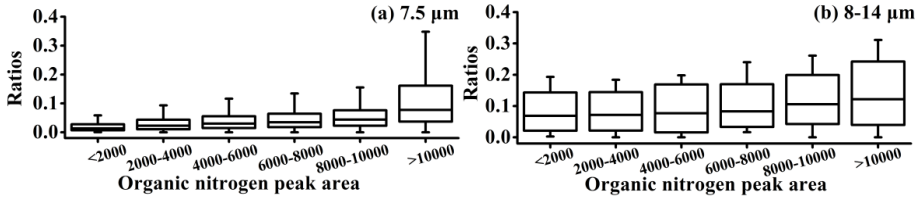

671

672 Figure 5

673

674